

## PUBLISHED VERSION

Zebrowski, J. J.; Grudzinski, K.; Buchner, T.; Kuklik, Pawel; Gac, J.; Gielerak, G.; Sanders, Prashanthan; Baranowski, R.

Nonlinear oscillator model reproducing various phenomena in the dynamics of the conduction system of the heart, *Chaos*, 2007; 17 (1):015121-1-015121-11.

© 2007 American Institute of Physics. This article may be downloaded for personal use only. Any other use requires prior permission of the author and the American Institute of Physics.

The following article appeared in *Chaos* **17**, 015121 (2007) and may be found at <http://link.aip.org/link/doi/10.1063/1.2405128>

### PERMISSIONS

[http://www.aip.org/pubservs/web\\_posting\\_guidelines.html](http://www.aip.org/pubservs/web_posting_guidelines.html)

The American Institute of Physics (AIP) grants to the author(s) of papers submitted to or published in one of the AIP journals or AIP Conference Proceedings the right to post and update the article on the Internet with the following specifications.

On the authors' and employers' webpages:

- There are no format restrictions; files prepared and/or formatted by AIP or its vendors (e.g., the PDF, PostScript, or HTML article files published in the online journals and proceedings) may be used for this purpose. If a fee is charged for any use, AIP permission must be obtained.
- An appropriate copyright notice must be included along with the full citation for the published paper and a Web link to AIP's official online version of the abstract.

31<sup>st</sup> March 2011

<http://hdl.handle.net/2440/43563>

## Nonlinear oscillator model reproducing various phenomena in the dynamics of the conduction system of the heart

J. J. Żebrowski, K. Grudziński, T. Buchner, P. Kuklik, and J. Gac

*Physics of Complex Systems Division, Faculty of Physics, Warsaw University of Technology, ul. Koszykowa 75, 00-662 Warszawa, Poland*

G. Gielerak

*Military Medical Institute, ul. Szaserów 128, Warszawa, Poland*

P. Sanders

*Cardiovascular Research Center, Royal Adelaide Hospital and the University of Adelaide, Adelaide, South Australia*

R. Baranowski

*Institute of Cardiology, ul. Alpejska 42, Warszawa, Poland*

(Received 31 July 2006; accepted 15 November 2006; published online 30 March 2007)

A dedicated nonlinear oscillator model able to reproduce the pulse shape, refractory time, and phase sensitivity of the action potential of a natural pacemaker of the heart is developed. The phase space of the oscillator contains a stable node, a hyperbolic saddle, and an unstable focus. The model reproduces several phenomena well known in cardiology, such as certain properties of the sinus rhythm and heart block. In particular, the model reproduces the decrease of heart rate variability with an increase in sympathetic activity. A sinus pause occurs in the model due to a single, well-timed, external pulse just as it occurs in the heart, for example due to a single supraventricular ectopy. Several ways by which the oscillations cease in the system are obtained (models of the asystole). The model simulates properly the way vagal activity modulates the heart rate and reproduces the vagal paradox. Two such oscillators, coupled unidirectionally and asymmetrically, allow us to reproduce the properties of heart rate variability obtained from patients with different kinds of heart block including sino-atrial blocks of different degree and a complete AV block (third degree). Finally, we demonstrate the possibility of introducing into the model a spatial dimension that creates exciting possibilities of simulating in the future the SA the AV nodes and the atrium including their true anatomical structure. © 2007 American Institute of Physics.

[DOI: [10.1063/1.2405128](https://doi.org/10.1063/1.2405128)]

**Human heart rate is not constant. In fact, heart rate variability is a major factor in the effective functioning of the cardiovascular system and an important factor in medical diagnosis. A large effort has gone into defining complexity measures using both chaos theory and statistical physics concepts in order to create tools for such diagnosis. In spite of this, the source of the variability is not completely understood and remains an open research subject. It is well known that the autonomous nervous system moderates heart rate in mammals. One way to understand how this occurs is to build models. A variety of models—including the so-called whole heart models—exist today. However, usually such models are so complex that an investigation of the global dynamical properties of the heart is difficult. Consequently, very rarely do they address the problem of heart rate variability. In our approach, we return to the 20th Century attempts of van der Pol and van der Mark of using relaxation oscillators to study the conduction system of the heart and its interaction with the autonomous nervous system. Following the work of several groups in the field, we developed our own modified van der Pol oscillator. We show that it is able to reproduce certain phenomena that occur in clinically recorded human heart rate: irregular heart rate,**

**asystole, sinus pause, vagal paradox, certain kinds of heart block, and others. The model may be extended into more than one dimension, which opens an interesting line of research.**

### I. INTRODUCTION

At present, the majority of models in mathematical biology pertaining to the heart and its function are formulated at the cellular level and take into account the details of the function of ion channels in the cell membrane.<sup>1</sup> This leads to a large number of nonlinear differential equations stemming from the Hodgkin-Huxley equations<sup>2</sup> of 50 years ago. As the number of parameters of each equation is also large and the dependence of the properties of the channels on the cell membrane potential complicated, the parameter space of this class of models is often very large, which makes difficult its analysis. In addition, the detailed properties of the various ion channels need to be determined in separate experiments and many properties are still to be uncovered. This class of models has made very important progress in recent years, and many important results including those related to new drugs have been found.

The aim of this paper is to study the possibility of forming a model of the conduction system of the heart, based on nonlinear oscillators and not on the properties of ion channels. The model should be able to reproduce the main properties of the system. The phenomenological approach using nonlinear oscillators is not suitable for the investigation of the cardiac conducting system at a cellular level but it allows a global analysis of heartbeat dynamics by investigating interactions between the elements of the system. We are interested in finding a simple model in order to ascertain what is the minimal structure of the phase space that allows the model to perform similarly to the conduction system of the heart. The conducting system of the human heart—the SA node (the primary pacemaker), the AV node, and the His-Purkinje system—may be treated as a network of self-excitable elements. These elements may be modeled as interacting nonlinear oscillators.<sup>3</sup> In the past, nonlinear oscillator models of heartbeat dynamics (see the paper by di Bernardo<sup>4</sup> and references therein) assumed bidirectional coupling between the SA and AV nodes. Such a coupling signifies that the SA node reacts immediately to the dynamics of the AV node. In our model of the conduction system, we assumed a unidirectional coupling between the nodes.

We based our model on the van der Pol (vdP) oscillator<sup>5</sup> given by

$$\frac{d^2x}{dt^2} + \alpha(x^2 - \mu)\frac{dx}{dt} + \omega_0^2x = F(t), \quad (1)$$

where  $\alpha$  is the damping constant,  $\mu=1$  for the van der Pol model, and  $\omega_0$  is the frequency. Note that  $x(t)$  may be expressed in volts if the parameters of Eq. (1) have the proper units (compare, e.g., Ref. 6). However, in the final section we discuss a model of the nodes SA and AV coupled to a FitzHugh-Nagumo equation as a model of the heart tissue. Since the variables of the FitzHugh-Nagumo equations are unitless, the variables describing the nodes were also made unitless throughout the paper. For convenience, we assumed such a (unitless) time scale so that the resultant magnitude of the periods of the oscillations may be compared with the magnitude of the periods observed in physiology.

We based our model on relaxation oscillators for two reasons:

First, the van der Pol oscillator adapts—without changing the amplitude<sup>7</sup>—its intrinsic frequency to the frequency of the external driving signal  $F(t)$ . This is a very important feature because the main cardiac pacemaker is the element of the conducting system with the highest frequency to which all other oscillators must adjust. As a result, a hierarchy of pacemakers in the conduction system of the heart is created, an observation that led van der Pol and van der Mark to the first model of the heart<sup>5</sup> based on Eq. (1).

Second, FitzHugh<sup>8</sup> showed that an extended version of the van der Pol equation (1) may be obtained as a simplification of the Hodgkin-Huxley equations. The FitzHugh-Nagumo model<sup>8</sup> may be treated as a link between relaxation oscillator models and modern analysis of physiological oscillators based on ion channels as, e.g., Ref. 1. Currently, both FitzHugh-Nagumo and Hodgkin-Huxley type models are used to study the properties of cardiac tissue.<sup>1</sup>

Since the work of van der Pol and van der Mark,<sup>5</sup> other models using relaxation oscillators<sup>6,8–10</sup> have been published. These models were mainly focused on the interaction between the AV and SA nodes. Although they provided many interesting results, they were not able to reproduce some important features of real cardiac action potentials. The most important of these features are the shape as well as the properties of the refractory period and are today reproduced by ion channel models such as those discussed in Refs. 1 and 11.

In Ref. 12, we introduced an oscillator that is more physiologically accurate in the sense of the shape of the action potential, the properties of the refractory period, and the possible ways of frequency change. Below, we show that it has interesting properties under different kinds of external drive and enables us to reproduce some important physiological phenomena. Contrary to what one may expect, we found that important results are due to the properties of the single oscillator. Consequently, a considerable space below is assigned to that aspect. The properties of the coupled oscillators as models of the interacting SA and AV nodes follow.

## II. THE MODEL

### A. Model of the isolated node

An action potential (AP) of a cell is generated when its membrane is excited above a certain threshold potential and ion channels are activated.<sup>13,14</sup> This allows ion currents to flow into or out of the cell, thus changing its potential and resulting in the generation of an action potential. After the discharge, the membrane potential returns to its rest state and the cell awaits another excitation input. During the generation of the action potential, the cell is in the refractive phase, and for a certain time (the refractory time) it is resistant to external perturbation.

The cells of the nodes of the cardiac conducting system have the property of spontaneous depolarization,<sup>14</sup> i.e., they can repeatedly generate an action potential on their own, without an external input. Figure 1 is a schematic drawing of the action potential and shows how the change of period of the action potential may occur according to the current knowledge in cardiology.<sup>15</sup> Depending on how fast the depolarization proceeds, the cells have different rates of generation of the action potentials. Curve a in Fig. 1 depicts the

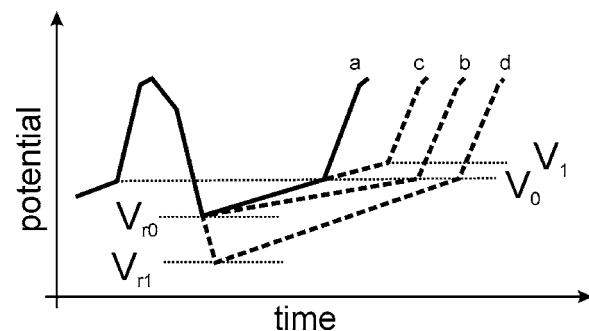


FIG. 1. Modes of change of action potential frequency: (a) original action potential, (b) change of depolarization time, (c) change of threshold potential from  $V_0$  to  $V_1$ , (d) change of resting potential  $V_{r0}$  to  $V_{r1}$ .

original action potential, while *b* depicts the one with a longer period due to an decrease of the depolarization rate. There are also other ways of regulating the firing frequency of the cardiac pacemaker:<sup>15</sup> through a change of the resting potential (curve *d* in Fig. 1) and through a change of the threshold potential from  $V_0$  to  $V_1$  (Fig. 1, curve *c*). These three mechanisms are very general and can be activated by many factors such as an increased activity of the sympathetic or of the parasympathetic nervous systems. They can also be related to physical damage to the conducting system.<sup>16</sup>

When constructing a model of the natural pacemaker of the heart, first of all we have to take into account two quantities: the time of spontaneous depolarization and the refractory time. The model should allow us to change these properties independently. Also, the ability to change the frequency of the model by incorporating the other two modes mentioned above is a desirable feature. It is well known that the classical van der Pol oscillator does not fulfill those conditions: changing the damping  $\alpha$  results in a simultaneous change of both the refractory and of the diastolic periods.

To study the synchronization of nonlinear oscillators, Postnov *et al.*<sup>18</sup> developed a modified van der Pol oscillator. In this oscillator, the harmonic force of Eq. (1) was replaced by a cubic (or Duffing) term,

$$\frac{d^2x}{dt^2} + \alpha(x^2 - \mu)\frac{dx}{dt} + x(x+d)(x+2d)/d^2 = 0, \quad d > 0. \quad (2)$$

Such a modification dramatically changes the properties of the system. Whereas the van der Pol oscillator had only a single unstable focus at  $x=0$ , the model of Ref. 18 has two more fixed points: a saddle at  $x=-d$  and a stable node at  $x=-2d$ , where  $d$  is a parameter.

The justification for making this modification given by the authors of Ref. 18 is that the phase space of the new system resembles the phase spaces of several physiological oscillators, e.g., that of the Morris-Lecar model of the neuron membrane.<sup>19</sup> For our model, however, an important effect of the modification is that the action potential is now biased toward negative values. This is the effect of the stable and unstable manifolds of the saddle in our system and is different from the van der Pol oscillator, where the action potential is always symmetric with respect to zero.<sup>12</sup> Also, with an increase of the parameter  $\mu$ , which controls the amplitude, the trajectory in our model changes its shape, becoming more curved as it passes the saddle. For a large enough  $\mu$ , the system undergoes a global homoclinic bifurcation, which results in the vanishing of the limit cycle and the trajectory resting at the stable node.<sup>18</sup>

The form of the model Eq. (2) implies that the distance between the saddle and the node cannot be changed. To be able to vary this distance, we introduced a new parameter  $e$  with both  $e$  and  $d$  positive,

$$\frac{dx_i}{dt} = y_i; \quad \frac{dy_i}{dt} = f(x_i, y_i), \quad (3)$$

$$f(x_i, y_i) = -\alpha_i(x_i^2 - \mu_i)y_i - f_i x_i(x_i + d_i)(x_i + e_i),$$

where  $\alpha$  is the damping constant and  $\mu$  is a constant usually set equal to 1. Now  $-e$  defines the position of the stable node

and  $-d$  is the position of the saddle. The parameter  $f$  allows us to adjust the frequency of the oscillator. The index  $i=1$  indicates the SA node while  $i=2$  indicates the AV node,  $x_i$  are the action potentials of the nodes, and  $y_i$  are the currents acting on these nodes. Our modification does not change the structure of the phase space of the system: in the phase space of the system, there will always be an unstable focus, a stable node, and a saddle.<sup>12</sup> Note that if  $e$  and  $d$  have opposing signs, the phase space of the system has the same structure as that of a Duffing oscillator, i.e., it contains an unstable focus and two saddle points.

Since one of our goals is to compare the results of the model with the heart rate variability data measured by 24-hour ECG, we took pains to keep the magnitude of the unitless frequency of the model within the range of the human heart rate. To facilitate this, we removed the term  $d^2$  (which becomes the product  $ed$  in our model) in the denominator of Eq. (2) and introduced the parameter  $f$ . An alternate way, which we also used, is to rescale the time. This latter approach introduces a constant into the model that is roughly equivalent to varying the capacitance in the Hodgkin-Huxley model and also changes the frequency of the oscillations.

As a further modification, we replaced the damping term  $\alpha(x^2 - \mu)$  in Eq. (3) by a term asymmetric with respect to the variable  $x$ :  $\alpha(x-v_1)(x-v_2)$  with  $v_1v_2 < 0$  to preserve the self-oscillatory character of the system (negative dissipation). Again, the phase space described above is preserved.

The action potential obtained<sup>20</sup> from the model of each single node Eq. (3) has the main properties of the action potential of the SA node measured in animal experiments: the shape, refractory time, and diastolic time (cf. Fig. 8 in Ref. 12). Although we did not do this here, the magnitude of the action potential may be easily rescaled to the physiological range. Note that by increasing the damping parameter  $\alpha$ , we extend the so-called phase 3 of the action potential. If we additionally make  $v_1v_2 > 0$ , then the model ceases to be self-oscillatory and Eq. (3) may be used as a model of the myocyte.

In our calculations, we set  $\alpha=5$ ,  $d=3$ ,  $v_1=1$ ,  $v_2=-1$ , and  $f=3$ . To model the SA node, we used  $e=12$ , and to model the AV node, we set  $e=7$ , in this way setting the proper ratio of the frequencies of the two nodes.

To compare simulation results with measured data, it is necessary to convert the generated action potentials to a heart rate signal. We assumed that action potentials of the AV node correspond to the contraction of the ventricles, thereby treating the effect of the His-Purkinje system as a simple delay. Thus, by measuring the intervals between consecutive AP spikes, we obtain interspike intervals (ISI) that can be compared with experimental data.

## B. Coupling the nodes

As both nodes of the conduction system of the heart have the property of automatism, assuming a diffusive coupling between them seems natural. However, we need to decide to which equation the diffusive coupling term should be attached, and whether this coupling should be unidirectional. A survey of the literature shows that in Refs. 4 and 6, a



bidirectional coupling term in the Eq. for the currents  $y_i$  was used. However, we decided to couple our oscillators unidirectionally adding the term  $(k_1x_1 - k_2x_2)$  to the equation for the potential of the AV node  $x_2$ . The coupling term may be interpreted as an additional current due to the difference between the action potentials of the two nodes, and it is in agreement with the formalism introduced originally by Hodgkin and Huxley.<sup>8</sup> A difference in the coefficients  $k_1$  and  $k_2$  allows us to introduce an asymmetry into the coupling, such as would be expected, for example, in a heart block.

### C. A spatially dimensional model of the SA node, atrium, and AV node

As will be shown below, the lumped model of Eq. (3) is able to produce interesting results and to reproduce some of the phenomena occurring in human heart rate variability. However, the conduction between the SA and AV nodes is a spatially extended process. To demonstrate that the nonlinear oscillator Eq. (3) is able to function in a spatially extended environment, we introduced a spatial dimension into our model. The SA and AV nodes were approximated by a one-dimensional (1D) chain of diffusively coupled oscillators each described by Eq. (3). The atrial muscle was modeled using a modified FitzHugh-Nagumo (FHN) model. The FHN model captures the key features of excitable media and is widely used as a simple model of cardiac muscle electrical activity.<sup>21</sup> The equations of the discretized FHN model are

$$\frac{dv_i}{dt} = \frac{1}{\mu} \left( v_i - \frac{1}{3}v_i^3 - u_i \right) + D_i(v_{i+1} + v_{i-1} - 2v_i),$$

$$\frac{du_i}{dt} = \mu(v_i + \beta - \gamma u_i),$$

where  $v_i$  is the activation variable (basically equivalent to the action potential) of the element  $\{i\}$ ,  $u_i$  is the total slow current at that element,  $\beta=0.7$ ,  $\gamma=0.5$ , and  $\mu=0.3$ . The diffusion coupling coefficient  $D_i$  was set to values between 10 and 60. The complete model consists of three segments: the SA node (15 elements), the atrial muscle (30 elements), and the AV node (15 elements) coupled diffusively at the interfaces (Fig. 2).

Since the activation variables in the models of the nodes (on the one hand) and in the model of the atrium (on the other hand) had different ranges of variability, a normaliza-

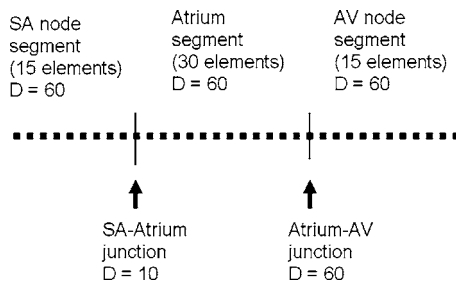


FIG. 2. Structure of the spatially extended model of the SA-AV pathway. The model is composed of three segments: SA node (15 elements), atrium area (30 elements), and AV node (15 elements). The grid elements at the interfaces are coupled diffusively.

tion should be performed at the interfaces between them. Linear transformations were applied to the activation variable in the diffusion coupling part of the equations so that the variables of both systems have the same minimum and maximum values. For example, the coupling term acting on an element at the interface on the SA side was

$$\text{coupling term} = D_{SA}(v_{i-1}^{SA} - v_i^{SA}) + D_{SA-A}(v^* - v_i^{SA}),$$

$$v^* = \frac{x_{\max}^{KG} - x_{\min}^{KG}}{v_{\max}^{FHN} - v_{\min}^{FHN}}(v_i^A - v_{\min}^{FHN}) + x_{\min}^{KG},$$

where  $D_{SA}=60$  and  $D_{SA-A}=10$  are the diffusion coupling coefficient at the SA node and the SA-atrium muscle interface, respectively. The index  $i$  marks the position of an element in the simulation grid.  $v^*$  is the activation variable on the atrial side of the system transformed linearly to fit the range of potentials within the node. Parameters  $x_{\max}^{KG}=1.56$ ,  $x_{\min}^{KG}=-2.4$ ,  $v_{\max}^{FHN}=1.8$ ,  $v_{\min}^{FHN}=-2.03$  are the extrema of the activation variables in both systems assessed numerically with the diffusion coupling set to zero. An analogical coupling method was used at the atria-AV node interface. Coupling at the atria-AV interface was varied to study the effect of the gap in the diffusion coefficient on conduction of the waves to the AV node.

The Euler integration scheme was used with a time step  $\Delta t=0.0001$ . We assumed zero-flux boundary conditions to minimize the effect of the chain ends. Note that following Ref. 21, we set the parameters of the FitzHugh-Nagumo equations in such a way so as to provide a physiologically plausible time scale of the action potential duration.

Extension of the model to a 1D chain geometry allows us to investigate the propagation of the activation waves. The abrupt change of the coupling constant assumed within the node-atria interface makes the system spatially inhomogeneous. Investigation of the propagation in the inhomogeneous system is important since it is believed that a conduction inhomogeneity in between the node and the atrial tissue plays a key role in the electrical protection of the nodes during episodes of atrial tachycardia.<sup>22-24</sup> The properties of the activation waves at the inhomogeneity were extensively studied in the past, and conditions for such wave propagation properties as wave block<sup>25,26</sup> or wave reflection<sup>27</sup> were found using ion channel models. The results obtained by our phenomenological model (Figs. 16-18) are in keeping with these general results.

## III. RESULTS AND DISCUSSION

### A. Properties of the single oscillator

Figure 3(a) depicts the action potential as a function of the time while Fig. 3(b) depicts the corresponding phase portrait. The curves are rendered by means of a dotted line with each dot representing a single time step of the numerical procedure. It can be seen that the passage close to the saddle occurs during the refractory period of the action potential. The dots are then very close to each other due to the critical slowing down of the trajectory close to the saddle. This is the same effect that results in the dephasing observed by

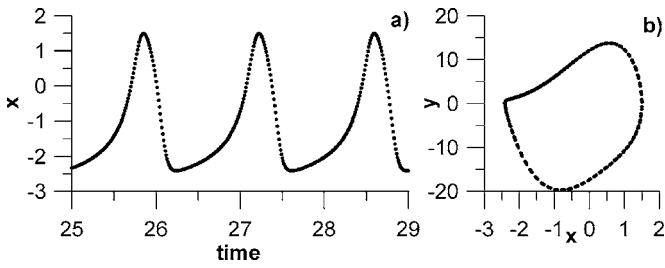


FIG. 3. Action potential as a function of the time (a) and the corresponding phase portrait (b). The points are plotted every numerical integration time step. Note that the state point slows down close to the saddle, i.e., during the refractory time.

Postnov.<sup>18</sup> Note that the position of the saddle affects the magnitude of the resting potential in our model.

By varying the position of the node (parameter  $e$ ), we change the frequency of the pulses (cf. Fig. 6 of Ref. 12). This is an important improvement with respect to the van der Pol oscillator: in the present case, *the shape of the action potential remains constant while the frequency may be changed in a wide range*. In effect, the change of parameter  $e$  in Eq. (3) results in a change of the rate of spontaneous depolarization, i.e., changing the diastolic period (curve b in Fig. 1).

The change of frequency is not linear, however. Figure 4 depicts the dependence of the period of the pulses  $T$  as a function of the position of the node  $e$ . It can be seen that the period saturates as the node moves away from the limit cycle and the pulse rate increases. For a model of the conduction system of the heart, this is an important property in accordance with the physiological properties of the heart: it is well known that the ability of the heart to increase its rate decreases at greater heart rates.<sup>16</sup> Also, physiological studies show that the activity of the sympathetic nervous system can increase the rate of the heart within a limited range.<sup>17</sup> Thus, the saturation of the curve depicted in Fig. 4 is consistent with physiological data and *an increase of the parameter  $e$  may be interpreted as a result of an increase of the activity of the sympathetic nervous system*.

The parameter  $\alpha$  changes the shape of the pulse, which results in a change of the refractory time. Thus, in our model, *we may manipulate the diastolic period and the refractory period independently*. The change of the shape of the action potential pulse may be large. Figure 3 depicts the action

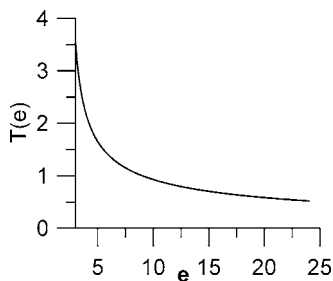


FIG. 4. The period of the oscillations  $T$  as a function of the parameter  $e$ . An increase of  $e$  corresponds to an increase of sympathetic activity. Note that, with an increase in  $e$ , a saturation of the oscillation period occurs and that a decrease of the variability is predicted.

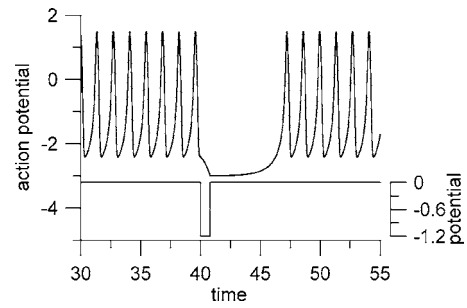


FIG. 5. Simulation of a pause due to the application of a single external negative pulse of the proper size and phase.

potential shape for  $\alpha=5$ , which is proper for a model of the potential of a node of the conduction system of the heart. However, if we set  $\alpha=25$ , we obtain a shape of the pulse that resembles the action potential of a myocyte<sup>14</sup> with a longer phase 3 of the action potential cycle.

Varying the parameters  $v_1$  and  $v_2$ , we were able to manipulate the frequency of the oscillator obtaining yet *another mechanism for the change of heart rate*. By varying the value of these parameters, we *lower or raise the value of the resting potential, thus decreasing or increasing the frequency of the generation of the action potentials, respectively* (curve d in Fig. 1). The important fact is that by an appropriate, simultaneous change of both parameters,<sup>12</sup> a change of the frequency may be obtained without changing the maximum value of the action potential (cf. Fig. 7 in Ref. 12).

### 1. Application of a single external pulse

It is well known that application of a single pulse to a limit cycle oscillator may result in a change of phase.<sup>6</sup> In particular, depending on the phase at which the external pulse is applied, the pulse of the oscillator may be delayed or occur prematurely. However, in the model discussed here the existence of the saddle introduces a new feature. First of all, an equivalent of the sinus pause may occur lasting much longer than the normal period of the isolated oscillator. In Fig. 5, the upper curve depicts the oscillation obtained from the model with the parameters set so that the period was nominally 1.3. The lower curve depicts the perturbation potential added to the equation for the potential and having a width of 0.8. It can be seen that the effect of the single pulse was such as to cause a pause 7.6 in length, in effect equivalent to a pause in the beating of the heart. Figure 6 depicts an ECG trace recorded in a patient who had a single supraventricular ectopic beat (arrow). This beat affected the sinus node and, as a result, the pause occurred (the pause in Fig. 6 lasted over 2 s).



FIG. 6. ECG trace with an example of a sinus pause. Arrow indicates a single supraventricular ectopic beat that resulted in a well visible pause in the activity of the sinus node.

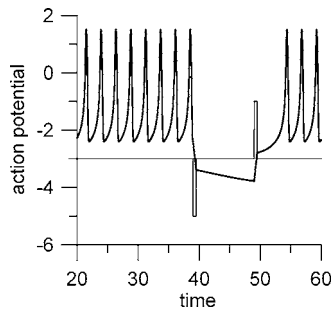


FIG. 7. A well-timed single negative pulse (thin line) results in the state point arriving at the stable node positioned at  $v = -4$  (thick line). The application of the subsequent positive pulse reverts the state point to the limit cycle.

When the perturbation pulse amplitude was increased by a very small amount (from  $-1.2$  to  $-1.205$ ) then the state point was forced over the saddle onto the stable node, resulting in an asystole. This is shown in Fig. 7, which also shows that the situation is reversible—the rhythm of the model may be regained by a later application of an appropriate positive pulse.

## 2. Effect of an external periodic pulse excitation

In general, the application of periodic pulses to the single oscillator results in an irregular response. This is due to the phase sensitivity of the system. Thus, when the first pulse is applied and occurs during the period of vulnerability of the oscillator, then the action potential will be delayed. The value of this delay is nonlinearly dependent on the phase of the external pulse and on its width and height. Examples of the phase response curve of the oscillator Eq. (3) are shown in Fig. 8 for different amplitudes of a single rectangular pulse train applied with a constant pulse width of 0.05. The zero of the phase was set at the maximum of the action potential. It can be seen that the phase response curve is continuous. For certain ranges of the phase of the input pulse, the slope of the curve changes rapidly so that a nonlinear response of the system is to be highly expected.

An example of an irregular pulsing resulting from an external periodic drive is shown in Fig. 9. This is also an effect of the nonlinear phase response curve. Nollo *et al.*<sup>29</sup> observed experimentally a variability of the period of the AV node action potential when the right atrium was kept under

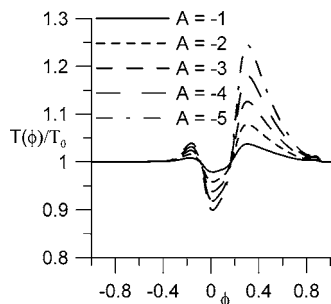


FIG. 8. The phase transition curve of the oscillator for several different amplitudes  $A$  of the single rectangular external pulse. The pulse width was 0.05.

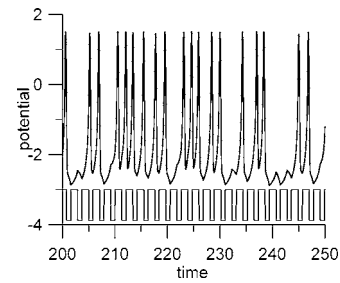


FIG. 9. Irregular response of the single node (thick line) due to the application of a regular square wave (thin line). The applied square wave had an amplitude of  $-0.88$ .

periodic stimulation so that the SA node was deactivated. The variability observed was low—of the order of 2%. They attributed this effect to a persistent modulation of the AV node by the autonomic nervous system. However, our results suggest that the variability observed may be due to the nonlinear oscillator properties of the AV node under the combined effect of the periodic pacing and the autonomic modulation.

The application of a train of periodic or even nonperiodic negative pulses to the model of the single node results in an increase of the average period of the oscillations. The modulation of the average pulse rate lasts as long as the train of negative pulses is applied. *This is in fact another way to modify the frequency of the node other than the ones usually described in textbooks<sup>15</sup> and summarized in Fig. 1.* Numerous examples of such changes of the heart rate occurring within a limited time may be found in 24-hour ECG recordings but are usually attributed to vagal activity (respiratory sinus arrhythmia).

A negative periodic input may result in a cessation of the oscillations (an asystole) of the single node. We applied a slow square wave of negative pulses to our model: the width of the pulses was 1 and the period was 6. When the amplitude was increased to 1.5, the trajectory was flipped across the saddle and ended in the stable node (cf. Fig. 3 of Ref. 28). Due to a fast response time, the oscillator reacts only to the last pulse of the square wave, so the effect is the same as for a single pulse applied at the right phase, as in Fig. 7. If the frequency of the square wave is larger than that of the oscillator, then also an asystole may occur because the effect of several pulses of the wave accumulates.

## B. Vagal paradox

Application of a properly shaped negative external pulse may be taken as a model of the action of acetylcholine: this hormone is associated with the activity of the vagal nerve, its ejection time is very short (i.e., the rise time of the pulse modeling it should be large), and it spontaneously decays relatively quickly (Ref. 30 and references therein). A train of such pulses may be used to model a number of phenomena that occur in the cardiovascular system. For example, a train of periodic pulses may model the effect of breathing that is mediated through the parasympathetic nervous system and so through pulses of the concentration of acetylcholine.



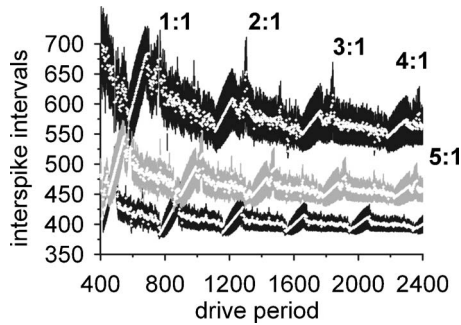


FIG. 10. Simulation of the vagal paradox: upper curve for  $e=3.5$  (black line), middle curve  $-e=6$  (gray line), lower curve  $-e=20$  (black line). Increase of the value of  $e$  models an increase in sympathetic activity while a decrease of the period of the drive models an increase of vagal activity.

The phenomenon called “vagal paradox” is another effect of the adaptation of the frequency of the oscillator to a train of negative pulses. It is usually expected that a larger intensity of the parasympathetic (i.e., vagal) activity results in a slower heart rate. It was shown, however, both in animal experiments<sup>30</sup> and by means of an ion channel model of the pacemaker cell,<sup>31</sup> that, depending on the parasympathetic activity (i.e., of the frequency of the negative pulses applied to the cell), the resulting oscillation period may vary in a nonmonotonous manner.

We reproduced this nonmonotonous behavior in our nonlinear oscillator model.<sup>32</sup> Figure 10 depicts the interspike intervals obtained in our model as a function of the period of the short negative spikes added to the current  $y_1$  in Eq. (2) for the following parameter values:  $\alpha=3$ ,  $d=3$ ,  $v_1=0.83$ , and  $v_2=-0.83$ ,  $d=3$  and  $e$  is a variable. The period of the negative spikes was changed from 0.4 to 4. Each spike had an instantaneous rise time and a fast exponential decay described by the equation  $-0.5 \exp(-\frac{t}{\tau})$  with  $\tau=50$  so that it decayed much earlier than the next spike that appears. Note that the frequency of the drive pulses applied in Fig. 10 was usually lower than the spontaneous frequency of the oscillator. The numerical experiment was repeated for three values of the position of the stable node (upper black curve  $e=3.5$ , gray curve  $-e=6$ , and lower black curve  $-e=20$ ). As discussed above, *increasing of the parameter  $e$  allows us to simulate an increase of the activity of the sympathetic branch of the autonomous nervous system*. A decrease of the period of the applied spike train simulates the effect of *an increase of vagal activity*. The white dots superimposed on each of the three curves in Fig. 10 depict the average ISI of the oscillator output as a function of the drive period. Due to the phase sensitivity of the oscillator (Figs. 8 and 9), its response frequency is not a constant and its variability is represented by the vertical width of each curve in Fig. 10.

If we focus on one of the three curves visible in Fig. 10, it may be seen that the mean oscillatory period is—to a first approximation—a decreasing function of the period of the external drive. However, for certain ranges of the drive frequency, both average periods become proportional to each other and the coupling ratio between both rhythms forms a sequence belonging to the Farey tree (mode-locking<sup>7,33</sup>). The coupling ratios 1:1, 2:1, ..., 5:1 are marked in Fig. 10.

Other straight line sections may be found in the graph and signify other, more complex mode-locking such as 3:2 (not marked). The width of a mode-locking region depends on the value of the parameter  $e$ . The results depicted in Fig. 10 show that our model is able to reproduce the vagal paradox.

Another important physiological feature reproduced by our model is that the change of the ISI due to a given change of the drive period depends on the value of the parameter  $e$  (Fig. 10). For higher values of  $e$ , i.e., a higher level of the sympathetic activity, the amplitude of the variability of the oscillator rhythm induced by the vagal activity is the smallest, i.e., the curve in Fig. 10 becomes flat. This effect is probably responsible for the well known phenomenon that the standard deviation of the RR intervals increases with the mean RR interval.<sup>16</sup>

Kotani *et al.*<sup>34</sup> introduced the term “mode locking” to describe the oscillatory response to the periodic (vagal) output in a modified Seidel-Herzel model. One important difference between their findings and the results shown here is that they introduced a feedback of the heart rhythm onto the breathing (or vagal) rhythm, in fact introducing a bidirectional coupling. We show that mode locking itself appears in our model under much weaker conditions, i.e., when only a unidirectional information flow occurs, from the vagal rhythm to a single node of the heart conduction system. The question of what is the exact nature of the coupling between breathing and heart rhythm—bi- or unidirectional—is beyond the scope of the current paper.

### C. Parametric modulation of the parameters of the single oscillator: Type I intermittency

In this section, we add to the oscillator developed above a periodic parametric drive. In terms of physiological processes, such a parametric forcing represents a time-dependent change of the working conditions of a pacemaker. We show that such a periodically forced system is able to exhibit type I intermittency.

Let us consider the equation of oscillator in the form of Eq. (3) with the values of parameters  $\alpha=3$ ,  $v_1=0.83$ ,  $d=3$ , and  $e=6$ . We now make the value of parameter  $v_2$  depend on the time,

$$v_2(t) = -0.83 \cdot [A \sin(\omega t)], \quad (4)$$

where  $\omega=0.802$  and  $A=0.1$ . Note that changing the relaxation parameter  $v_2$  changes both the frequency of the action potential and its amplitude.<sup>12</sup> The parametric drive Eq. (4) causes an irregular behavior of the oscillator. Figure 11 presents the time series of every third interval obtained with the parametric drive. It can be seen that for relatively long periods of time, these intervals lie close to a period-3 orbit (laminar phases) and these periods of time are separated by chaotic bursts. During the laminar phase, the value of the intervals is nearly constant, monotonically increasing or monotonically decreasing at the end of the phase. This indicates type-I intermittency.<sup>35,36</sup> Also, the laminar phase distribution, presented in Fig. 12, has two peaks (at the minimum and maximum laminar phase length), very characteristic for this type of intermittency.



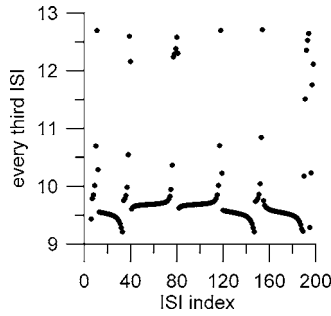


FIG. 11. Every third ISI obtained during parametric forcing of the oscillator. During laminar phases the system is close to a period-3 orbit.

However, intermittency in this system is somewhat different from that observed in many unimodal maps such as the logistic map. The map constructed from the data in Fig. 11 oscillator is depicted in Fig. 13. The behavior of the system is more complex than in the case of a unimodal map: we obtained a torus typical for quasiperiodicity induced by the parametric drive. The torus is shaped so that it approaches tangency to the diagonal at three points resulting in type I intermittency.

Type I intermittency has been reported in human heart rate variability.<sup>36,37</sup> This phenomenon seems to occur for different types of pathology: it is often found for cases of ventricular arrhythmia but also for certain cases of atrial fibrillation. The varied nature of the pathologies with which it is associated indicates that the intermittency may be associated with the conduction system of the heart. It is interesting that in our model of the single node, it is surprisingly easy to obtain type I intermittency in the dynamics of the interspike interval. Note, however, that the laminar phase distribution found in Refs. 36 and 37 is not like the textbook example shown in Fig. 11. It has been known for a long time that additive noise may distort the right peak of the distribution and make it narrower.<sup>38</sup> Recently, it was shown analytically<sup>39</sup> that nonstationarity may result in the right peak of the distribution splitting into two or three peaks. References 36 and 37 describe numerical experiments in which the laminar lengths distribution was made wider by parametric random noise and the right peak was weakly defined. Preliminary numerical experiments using the oscillator described here show that introducing nonstationarity into the parametric

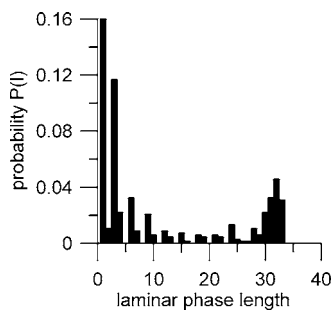


FIG. 12. Probability distribution of the laminar phases during intermittency induced by parametric forcing of the parameter  $v_2$ .

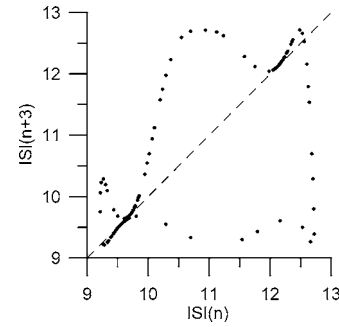


FIG. 13. The map obtained from the data in Fig. 11.

modulation results in laminar phase distributions comparable with the ones obtained in human heart rate variability.<sup>36,37</sup> This will be the subject of a separate report.

Periodic modulation of the parameter  $e$  which defines the position of the stable node also leads to the occurrence of intermittency in the interspike intervals of the action potential series. It appears that the observed phenomena are more intricate than in the case of the modulation of the relaxation parameter  $v_2$  described above and require more investigation.

#### D. Coupled oscillators

To simulate the interaction of the SA and the AV nodes, we used the two oscillators described by Eq. (3) and coupled them by adding the term  $k_1x_1 - k_2x_2$  to the equation for the AV node. At first we assumed that  $k_1 = k_2 = 1$  and chose the parameters of the model so that the intrinsic frequencies of the nodes were 1.1 and 0.75, respectively. With such a setting, the slower oscillator mode locks to the faster one, just as it happens in the system composed of the SA node and the AV node within the heart. With the frequency of the AV node oscillator held constant and increasing the frequency of the SA node in the model, more complex mode-locked behaviors of different rational ratios were obtained including 2:1, 3:2, and other. For large frequencies of the SA node and the AV node, the response became chaotic.

##### 1. Model of a sino-atrial heart block

Changing the magnitude of the constant  $k_2$  with respect to that of  $k_1$  leads to effects very similar to a 3:2 sino-atrial heart block.<sup>28</sup> Part (a) of Fig. 14 depicts the Poincaré map of the data [part (c)] measured in the patient LTK, while parts (b) and (d) depict the corresponding result of the simulation for  $k_1 = 0.75$  and  $k_2 = 0.5$ . Note that, both in the measured data and in the simulation, the points of the map form a curve starting at the diagonal and oriented upwards on the graph. This feature is an indication of quasiperiodicity. Note that in clinical practice, it is very difficult to ascertain that quasiperiodicity has occurred in the data as the type of block is determined by finding in the ECG trace an integer ratio of the number of  $P$  peaks to the number of QRS complexes.

We were also able to simulate a more complicated case of the sino-atrial block: a mixture of a 3:2 and a 2:1 block.<sup>28</sup> This resulted in an escape rhythm sporadically interrupted by the sinus rhythm. This case was simulated by assuming the

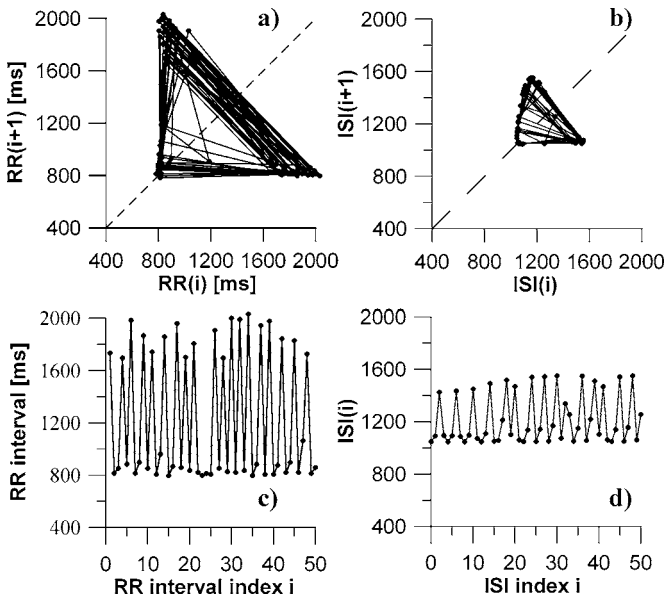


FIG. 14. 3:2 sino-atrial block. Left panels depict the heart rate variability data and Poincaré map measured in an ECG recording of a patient with a second degree block. The two right panels show the results of the model obtained for  $k_1=0.75$  and  $k_2=0.5$ .

same value for both coupling constants but switching the coupling off for 14 s (approximately ten periods of the AV node) and switching it on for 1.15 s (approximately one period of the SA node).

**2. Amplitude death due to coupling imbalance**

If the constant  $k_2$  was set equal to zero or very small (i.e., the coupling becomes a master-slave configuration, e.g.,  $k_1=0.75$  and  $k_2 < 0.19$ ), amplitude death (cessation of the oscillations) occurred. The state point of the AV node oscillator approached the saddle and was then attracted onto the stable fixed point (Fig. 15). Setting  $k_2$  to very low values models the essential features of a disease of the AV node or of the tissue surrounding it (e.g., the complete AV block of the third degree<sup>16</sup>).

**E. Adding a spatial dimension to the model**

Figures 16–18 depict the wave shapes of the action potentials obtained for the spatially extended model of the SA

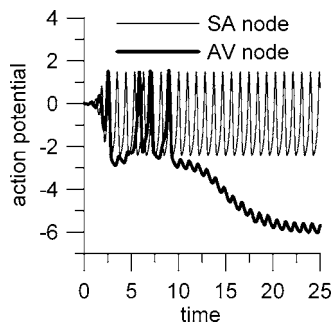


FIG. 15. Amplitude death (asystole) at the AV node (thick line) due to a strong asymmetry of the diffusive coupling. The node was coupled to the SA node, which remained active (thin line).

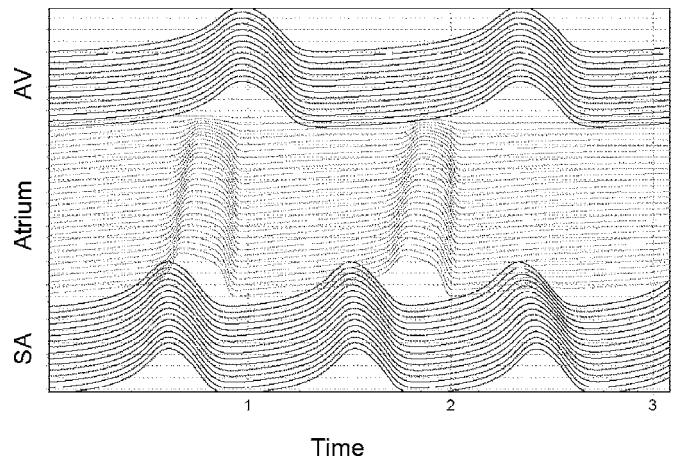


FIG. 16. Simulated wave shapes for  $D_{SA-A}=0.1$  and  $D_{A-AV}=0$  resulting in a delayed depolarization of the atrium in the first two activations and conduction block during the third activation.

node-atrium-AV node system as functions of the time. The black curves at the bottom of the figures denote elements of the SA node, middle gray curves denote action potential in the atrium, and the black curves at the top denote elements of the AV node. The time flows to the right.

Figure 16 depicts the conduction of the action potentials for the coupling parameter at the SA-atrium interface  $D_{SA-A}$  set equal to 0.1 and at the AV-atrium interface  $D_{A-AV}$  to 0 (complete block). Such low coupling results in a delayed depolarization of the atrium during the first two activations and a conduction block after the third activation of the SA node. The delay observed is caused by the inhibition of the depolarizing effect of the SA node on the elements of the atrium caused by a low coupling at the interface. The conduction block after the third activation is due to the repolarization phase of elements of the atrium during the activation of the SA node. The AV node remains self-oscillatory.

When the coupling between at the SA-atrium interface was increased to  $D_{SA,A}=10$ , the interface was able to conduct

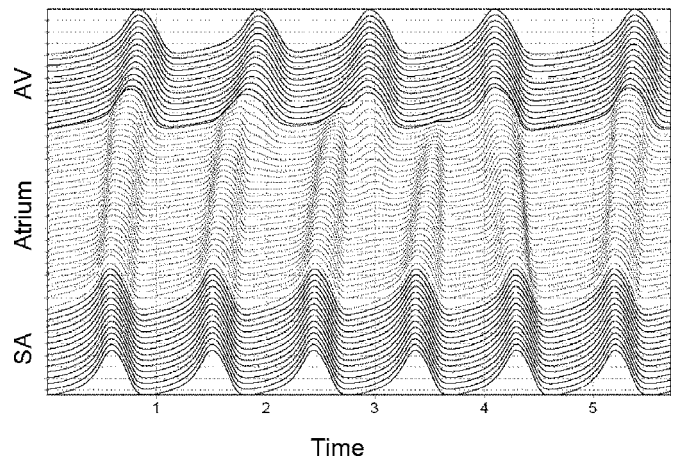


FIG. 17. Simulated wave shapes for the diffusion coefficient at both interfaces set equal to 10 ( $D_{SA,A}=10, D_{A-AV}=10$ ). Such a coupling strength results in a 1:1 conduction between the SA and the atrium, but the activation wave is unable to depolarize the AV node, which results in a lack of synchronization between the SA and the AV nodes.

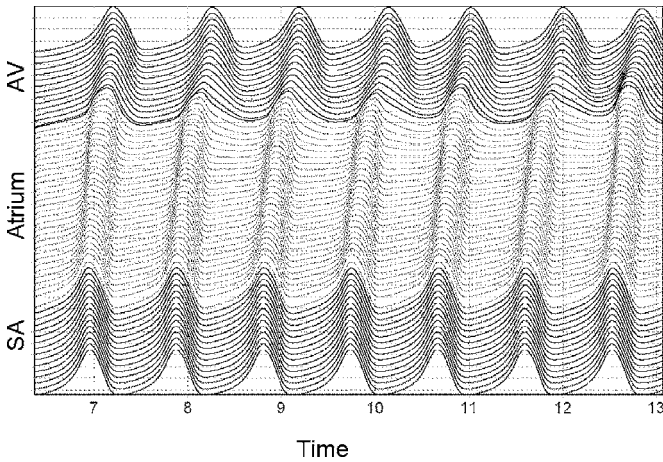


FIG. 18. Simulated wave shapes for  $D_{SA,A}=10$  and  $D_{A,AV}=60$ . In this case, the coupling at the atrium-AV interface is strong enough to enable synchronization of both nodes with the frequency of the SA node.

in a 1:1 fashion into the atrium without delays (Fig. 17). Setting such a coupling at the AV-atrium interface ( $D_{A,AV}=10$ ) was not enough for the activation wave to depolarize the AV node. This results in a lack of 1:1 synchronization between the SA and the AV nodes. Because of the inability of the SA node to excite the AV node, a retrograde conduction occurred (fourth activation of the AV node in Fig. 17).

In order to obtain a complete synchronization between both nodes, the coupling at the AV-atrium interface was increased to 60 ( $D_{SA,A}=10, D_{A,AV}=60$ ). A 1:1 synchronization between the SA and AV nodes was observed with the SA node acting as a pacemaker for the whole system (Fig. 18).

#### IV. CONCLUSIONS

A new oscillator model that reproduces the main properties (the action potential shape, the refractory time, and the diastolic period) of the action potential of a natural pacemaker of the heart was developed. The phase space of the oscillator contains a stable node, a hyperbolic saddle, and an unstable focus. Such a structure of the phase space seems to be the minimum one that allows us to model several properties of the conduction system of the heart observed experimentally. The period of oscillations saturates as the node moves away from the limit cycle; in our model, this is due to a change of the parameter that may be associated with sympathetic activity. This property of the node reproduces two well known properties of the heart rate and its variability: (a) sympathetic activity will not increase the heart rate to an indefinitely large magnitude and (b) the heart rate variability decreases with an increase in sympathetic activity. A pause in the oscillations occurs in the model due to a single well-timed external pulse just as it occurs in the heart due to a single supraventricular ectopy. A slightly larger negative pulse may place the state point at the stable node (cessation of oscillations) and a subsequent positive pulse switches the oscillations back on. Similar phenomena occur in the heart as a result of, e.g., electrocution and subsequent defibrillation. The model of the node exhibits a homoclinic bifurcation, which may also lead to an asystole.

Because the phase response curve of the oscillator is highly nonlinear, a regular square wave drive results in an irregular response with an average period lower than the spontaneous one. This simulates how the vagal branch of the autonomous nervous system modulates the heart rate. This mode of frequency change is different from the three modes usually described in physiology textbooks<sup>14,15</sup> where the sinus node changes its frequency through a change of the threshold potential, of the rate of spontaneous depolarization, or of the resting potential. The model also reproduces the vagal paradox,<sup>30,31</sup> which is a complex interplay of the activity of the sympathetic and the vagal activities.

Two oscillators coupled unidirectionally and asymmetrically allow us to reproduce the properties of heart rate variability obtained from patients with different kinds of heart block including sino-atrial blocks of a different degree and a complete AV block (third degree).

We demonstrated the possibility of extending the model by adding a spatial dimension. This allows the investigation of such properties of the SA and AV nodes, which are due to the spatial nature of the system (e.g., retrograde conduction and the effect of the properties of the node-atrium interface on wave propagation). We are developing a three-dimensional model of the SA, the AV nodes, and the atria based on the true anatomical geometries<sup>40</sup> derived from computer tomography images, including the anisotropy and fiber structure as well as the viability of the tissue taken from electrophysiological measurements and tomography.

Initially, we expected that a successful model of the single node of the conduction system of the heart will be only the first step, and that to obtain results observable in human heart rate variability recordings will require the inclusion of various external regulation mechanisms such as the baroreflex. We expect to see interesting results when the external regulatory mechanisms will be included in our model in the future.

We found, however, that several important properties observed in the human heart rate are due to the nonlinear properties of the single node. This seems an interesting result as the autonomic nervous system acts more strongly on the SA node than on the rest of the conduction system (the density of nerve endings is the largest in the vicinity of the SA node<sup>14</sup>).

The phenomenological model described here obviously may not reproduce all properties of the conduction system of the heart. For that, extensive models including many ion channels are needed. One interesting problem would be to compare the minimum phase-space configuration of our model with that of the successful ion channel models.

#### ACKNOWLEDGMENT

The paper was supported by the Polish Ministry of Science, Grant No. 134/E-365/SPB/COST/KN/DWM 105/2005-2007.

<sup>1</sup>J. Keener and J. Sneyd, *Mathematical Physiology*, Interdisciplinary Applied Mathematics 8 (Springer, New York 1998).

<sup>2</sup>A. L. Hodgkin and A. F. Huxley, "A quantitative description of membrane current and its applications to conduction and excitation in nerve," *J. Physiol. (London)* **117**, 500-544 (1952).



- <sup>3</sup>G. Bub and L. Glass, "Bifurcations in a discontinuous circle map: A theory for a chaotic cardiac arrhythmia," *Int. J. Bifurcation Chaos Appl. Sci. Eng.* **5**, 359–371 (1995).
- <sup>4</sup>D. di Bernardo, M. G. Signorini, and S. Cerutti, "A model of two nonlinear coupled oscillators for the study of heartbeat dynamics," *Int. J. Bifurcation Chaos Appl. Sci. Eng.* **8**, 1975–1985 (1998).
- <sup>5</sup>B. van der Pol and J. van der Mark, "The heartbeat considered as a relaxation oscillation and an electrical model of the heart," *Philos. Mag.* **6**, 763–775 (1928).
- <sup>6</sup>B. J. West, A. L. Goldberger, G. Rovner, and V. Bhargava, "Nonlinear dynamics of the heartbeat. The AV junction: Passive conduit or active oscillator?," *Physica D* **17**, 198–206 (1985).
- <sup>7</sup>J. M. T. Thompson and H. B. Steward, *Nonlinear Dynamics and Chaos* (Wiley, New York, 2002).
- <sup>8</sup>R. FitzHugh, "Impulses and physiological states in theoretical models of nerve membrane," *Biophys. J.* **1**, 445–466 (1961).
- <sup>9</sup>C. R. Katholi, F. Urthaler, J. Macy, Jr., and T. N. James, "Mathematical model of automaticity in the sinus node and the AV junction based on weakly coupled relaxation oscillators," *Comput. Biomed. Res.* **10**, 529–543 (1977).
- <sup>10</sup>J. Honerkamp, "The heart as a system of coupled nonlinear oscillators," *J. Math. Biol.* **18**, 69–88 (1983).
- <sup>11</sup>H. Zhang, A. V. Holden, I. Kodama, H. Honjo, M. Lei, T. Varghese, and M. R. Boyett, "Mathematical models of action potentials in the periphery and center of the rabbit sinoatrial node," *Am. J. Physiol. Heart Circ. Physiol.* **279**, H397–H421 (2000).
- <sup>12</sup>K. Grudziński and J. J. Żebrowski, "Modeling cardiac pacemakers with relaxation oscillators," *Physica A* **336**, 153–152 (2004).
- <sup>13</sup>*Theory of Heart*, edited by L. Glass, P. Hunter, and A. McCulloch (Springer-Verlag, Berlin, 1990).
- <sup>14</sup>*Cardiac Electrophysiology: From Cell to Bedside*, edited by P. D. Zipes and J. Jalife (Saunders, Philadelphia, 2000).
- <sup>15</sup>B. F. Hoffman and P. F. CraneField, *Electrophysiology of the Heart* (McGraw Hill, New York, 1960).
- <sup>16</sup>A. Bayés de Luna, *Clinical Electrocardiography: A Textbook* (Futura, 1998).
- <sup>17</sup>O-E. Brodde and M. C. Michel, "Adrenergic and muscarinic receptors in the human heart," *Pharmacol. Rev.* **51**, 651–689 (1999).
- <sup>18</sup>D. Postnov, K. H. Seung, and K. Hyungtae, "Synchronization of diffusively coupled oscillators near the homoclinic bifurcation," *Phys. Rev. E* **60**, 2799–2807 (1999).
- <sup>19</sup>C. Morris and H. Lecar, "Voltage oscillations in the barnacle giant muscle fiber," *Biophys. J.* **35**, 193–213 (1981).
- <sup>20</sup>The Dynamics Solver program, due to J. M. Aguirregabiria (<http://tp.lc.ehu.es/jma.html>), was used with the fourth-order Runge-Kutta method.
- <sup>21</sup>A. V. Holden and V. N. Biktashev, "Computational biology of propagation in excitable media models of cardiac tissue," *Chaos, Solitons Fractals* **13**, 1643–1658 (2002).
- <sup>22</sup>S. L. Cloherty, S. Dokos, and N. H. Lovell, "A comparison of 1-D models of cardiac pacemaker heterogeneity," *IEEE Trans. Biomed. Eng.* **53**, 164–177 (2006).
- <sup>23</sup>M. Boyett, M. R. Honjo, and H. I. Kodama, "The sinoatrial node, a heterogeneous pacemaker structure," *Cardiovasc. Res.* **47**, 658–687 (2000).
- <sup>24</sup>R. W. Joyner and F. J. L. van Capelle, "Propagation through electrically coupled cells: How a small SA node drives a large atrium," *Biophys. J.* **50**, 1157–1164 (1986).
- <sup>25</sup>T. J. Lewis and J. P. Keener, "Wave-block in excitable media due to regions of depressed excitability," *SIAM J. Appl. Math.* **61**, 293–316 (2000).
- <sup>26</sup>A. Kulka, M. Bode, and H. G. Purwins, "On the influence of inhomogeneities in a reaction-diffusion system," *Phys. Lett. A* **203**, 33–39 (1995).
- <sup>27</sup>G. B. Ermentrout and J. Rinzel, "Reflected waves in an inhomogeneous excitable medium," *SIAM J. Appl. Math.* **56**, 1107–1128 (1996).
- <sup>28</sup>K. Grudziński, J. J. Żebrowski, and R. Baranowski, "A model of the sino-atrial and the atrio-ventricular nodes of the conduction system of the human heart," *Biomed. Eng. (NY)* **51**, 210–214 (2006).
- <sup>29</sup>G. Nollo, M. Del Greco, F. Ravelli, and M. Disertori, "Evidence of low- and high-frequency oscillations in human AV interval variability: Evaluation with spectral analysis," *Am. J. Physiol.* **267** (Heart Circ. Physiol. 36), H1410–H1418 (1994).
- <sup>30</sup>J. Jalife, V. A. Slenter, J. J. Salata, and D. C. Michaels, *Circ. Res.* **52**, 642–656 (1983).
- <sup>31</sup>S. S. Demir, J. W. Clark, and W. R. Giles, *Am. J. Physiol. Heart Circ. Physiol.* **276**, H2221–H2244 (1999).
- <sup>32</sup>T. Buchner, G. Gielerek, and J. J. Żebrowski, *Proceedings of the European Study Group for Cardiovascular Oscillations ESGCO*, Jena 2006, pp. 191–194.
- <sup>33</sup>L. Glass, "Synchronization and rhythmic processes in physiology," *Nature (London)* **410**, 277–284 (2001).
- <sup>34</sup>K. Kotani, K. Takamasu, Y. Ashkenazy, H. E. Stanley, and Y. Yamamoto, "A model for cardio-respiratory synchronization in humans," *Phys. Rev. E* **65**, 051923 (2002).
- <sup>35</sup>P. Manneville and Y. Pomeau, *Phys. Lett.* **75A**, 1 (1979).
- <sup>36</sup>J. J. Żebrowski and R. Baranowski, "Type I intermittency in nonstationary systems—Models and human heart rate variability," *Physica A* **336**, 74–83 (2004).
- <sup>37</sup>J. J. Żebrowski and R. Baranowski, "Observations and modeling of deterministic properties of human heart rate variability," *Pramana* **64**, 543–562 (2005).
- <sup>38</sup>H. Hirsch, B. A. Huberman, and D. J. Scalapino, "Theory of intermittency," *Phys. Rev. A* **25**, 519–532 (1982).
- <sup>39</sup>J. M. Gac and J. J. Żebrowski, "Nonstationary Pomeau-Manneville intermittency in systems with a periodic parameter change," *Phys. Rev. E* **73**, 066203 (2006).
- <sup>40</sup>P. Kuklik, L. Szumowski, J. J. Żebrowski, and F. Walczak, *Physiol. Meas.* **25**, 617–627 (2004).